

## Size and distribution of Pt nanoparticles in LDH nanocomposites at different temperatures

D. B. Karashanova<sup>1\*</sup>, D. D. Kostadinova<sup>2</sup>, S. V. Vasilev<sup>2</sup>, N. L. Petrova<sup>3</sup>

<sup>1</sup> *Institute of Optical Materials and Technologies “Acad. Jordan Malinovski”,  
Bulgarian Academy of Sciences, 1113 Sofia, Bulgaria*

<sup>2</sup> *Institute of Electrochemistry and Energy Systems, Bulgarian Academy of Sciences, 1113 Sofia, Bulgaria*

<sup>3</sup> *Institute of Mineralogy and Crystallography, Bulgarian Academy of Sciences, 1113 Sofia, Bulgaria*

Received February 15, 2012; Revised April 17, 2012

Nanocomposites were successfully synthesized from multicationic layered double hydroxides (LDHs) and platinum nanoparticles (PtNPs). The features of the nanocomposite layer structure were characterized by XRD and IR analyses while the thermal behaviour by DTA-TG. The observed interlayer contraction can be explained by the grafting of interlayer organic anions onto the hydroxylated layers. The change of the mean size and the size distribution of the PtNPs after heat treatment of the samples at 500 °C and 1000 °C were observed by TEM. The intercalated in the support PtNPs were coalesced under heating. Spherical and highly dispersed nanoparticles were observed at room temperature while rough and granular aggregates were formed at 500 °C and large, dense and well-faceted particles at 1000 °C.

**Key words:** Pt-LDH nanocomposite, TEM of Pt nanoparticles, thermal treatment.

### INTRODUCTION

A recent review has shown the great potential of layered double hydroxides (LDHs) as precursors of metal particles on basic supports with very unique properties [1, 2], as regards metal-support interaction (“electron transfer”) and metal-support cooperation (“metal-base bifunctional catalysis”). It is known also that LDHs are good precursors for loading noble metals and non noble metals [3]. LDHs of general formula  $[M_{1-x}^{2+} M_x^{3+}(\text{OH})_2][A_{x/n}^{n-} \cdot m\text{H}_2\text{O}]$  can contain different  $M^{2+}$  and  $M^{3+}$  metal cations in their brucite-like sheets, and various  $A^{n-}$  charge-compensating anions in their interlayer space. LDH compounds easily decompose into mixed oxides of the  $M^{2+}M^{3+}(\text{O})$  type after calcination [4–6]. These materials have both basic and redox functions as catalysts.

Three general routes are available for synthesis of LDHs precursors: first, the synthesis of LDHs containing  $M^{2+}$  and/or  $M^{3+}$  elements with redox behaviour within the sheets; second, the exchange with anionic metal precursors of the desired metal

in the interlayer space of the LDHs; third, the deposition or grafting of inorganic or organometallic precursors onto the calcined precursor LDH. The advantage of the second route for synthesis is that the steric hindrance in the interlayer space prevents aggregation of the nanoparticles and allows the control of their growth. However these routes of catalysts preparation suffer from several limitations: (i) pure LDH phases cannot be obtained with a noble metal content larger than 5 at.% [7, 8]; (ii) catalytically active ions of too large ionic radius or without octahedral coordination cannot be accommodated in the brucite-like sheets [1, 4] and (iii) the sizes of the metal particles obtained after calcination and reduction of the LDH or mixed oxides are not easily controlled, aggregation often takes place leading to large particle sizes [9]. Keeping in mind these drawbacks, there is a demand to design new synthesis routes for obtaining highly loaded metal catalysts with control of noble metal particles in size and distribution starting from LDH precursors.

A recent report has described a novel preparation method of such materials by intercalation of preformed negatively charged Ni-based nanoparticles in Mg/Al LDH [10]. It has been shown that a better control of nanosized Ni<sup>0</sup> particles could be achieved. Three approaches are considered in order to prepare LDH nanocomposites incorporating

\* To whom all correspondence should be sent:  
E-mail: dkarashanova@yahoo.com

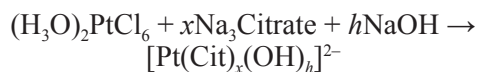
large negatively charged entities: the LDH co-precipitation and the reconstruction of the host LDH in the presence of the anionic species, and the anion exchange route of, for example, nitrate-containing LDH with the anions [10–11]. The first two methods yield poorly ordered layered structures, while the third yields well-ordered lamellar structures. Moreover, the anionic exchange route is the only one that allows us to tailor Ni particle sizes in the calcined and reduced materials.

The aim of the present work was therefore the preparation of highly disperse supported Pt-metal catalyst by intercalation of platinum nanoparticles into multicationic LDHs and fine control of the size and microstructure of Pt NPs at room temperature and after heat treatment at 500 °C and 1000 °C. For this purpose original Pt-containing LDH nanocomposites were prepared by exchange route of negatively charged Pt colloids with controlled sizes of the nanoparticles.

## EXPERIMENTAL

### *Preparation of Pt-Colloid*

Colloidal suspensions of Pt-based particles were obtained by hydrolysis of an aqueous solution of  $(\text{H}_3\text{O})_2\text{PtCl}_6$  (8%) and  $\text{Na}_3(\text{C}_6\text{O}_7\text{H}_3)$  (1%) with NaOH (4%). This modified method of synthesis is created on the basis of works of Turkevich [12] and Harriman [13]. The molar ratio  $x = [\text{citrate}]/[\text{Pt}]$  was 3.45. Hydrolysis of  $\text{Pt}^{2+}$  ions was performed at a controlled platinum hydroxylation ratio  $h = [\text{OH}]/[\text{Pt}] = 7.95$  at alkaline pH = 10 and temperature of 80 °C. The general equation of the reactions of formation of Pt-complex, followed by hydrolysis can be presented by:



### *Preparation of LDH Host Structure, Pt-LDH nanocomposite and its conformations after heat treatment*

(i) The host  $\text{NO}_3$ -Mg/Ni/Al sample (Mg/Ni/Al = 2:0.5:1) was prepared by co-precipitation at constant pH=10 of suitable amounts of  $\text{Mg}(\text{NO}_3)_2 \cdot 6\text{H}_2\text{O}$  (21.7%),  $\text{Al}(\text{NO}_3)_3 \cdot 9\text{H}_2\text{O}$  (15.8%) and  $\text{Ni}(\text{NO}_3)_2 \cdot 6\text{H}_2\text{O}$  (6.1%) with a solution of NaOH (4%). The addition of the alkaline solution was controlled by using a pH-STAT Titrino (Metrohm) apparatus to keep the pH constant. The suspension was stirred at 80 °C for 17 h, and then the solid fraction was separated by centrifugation, washed thoroughly with distilled

water and dried overnight at 80 °C [14]. These samples will be hereafter labeled  $\text{NO}_3$ -LDH.

(ii) The Pt-LDH nanocomposite was prepared from the  $\text{NO}_3$ -LDH by anionic exchange of nitrate ions: 0.6 g of the host  $\text{NO}_3$ -LDH was dispersed in the required amounts of a 2% aqueous suspension of Pt-based nanoparticles ( $[\text{citrate}]/[\text{Pt}] = 3.45$ ;  $([\text{OH}]/[\text{Pt}]) = 7.95$ ). The exchange process was performed by stirring the mixture in air at temperature of 80 °C for 6 h. The solid fraction was then recovered and washed by dispersion and centrifugation in distilled water and finally dried at 80 °C for 12 h.

(iii) Two conformations of the Pt-layered nanocomposite were obtained after heat treatment at 500 °C – mixed oxide Mg/Ni/Al(O) and 1000 °C – spinel  $\text{MgNiAl}_2\text{O}_4$  type phase.

### *Methods of characterization*

Phase identification was performed using powder XRD data obtained by XRD patterns recorded on a Bruker D8 Advance instrument using the  $\text{Cu K}\alpha_1$  radiation ( $\lambda = 1.542 \text{ \AA}$ , 40 kV, and 50 mA).

The infrared absorption spectra were measured with a Tensor 37, Bruker FTIR spectrometer in the MIR 400–4000  $\text{cm}^{-1}$  spectral range with a 2  $\text{cm}^{-1}$  spectral resolution, after averaging 72 scans on standard KBr pallets.

DTA-TG analyses were performed on Stanton Redcroft, STA 780 equipment operating at a heating rate of 10°  $\text{min}^{-1}$ , dynamic air conditions and  $\text{Al}_2\text{O}_3$  used as a reference.

The microstructure of the samples was investigated by means of HRTEM JEOL JEM 2100, operated at 200 kV accelerating voltage. For the phase composition identification Selected Area Electron Diffraction (SAED) was applied. Pt-LDH nanocomposite and thermally treated powders were dispersed in ethanol. Micro-quantities of the colloids were dropped on standard Cu TEM grids, coated with carbon and dried for subsequent observation.

## RESULTS AND DISCUSSION

### *Characterization of Pt-LDH nanocomposite*

*XRD patterns* of the host  $\text{NO}_3$ -LDH and of the Pt colloid-exchanged LDH are shown in Figure 1. In all cases the XRD patterns are typical for LDHs structures. The reflections can be indexed in a hexagonal lattice with a  $R3hm$  rhombohedral symmetry. The two sharp and intense characteristic diffraction lines appearing as symmetric lines at  $2\theta$  angles below 25 °C in the  $\text{NO}_3$ -LDH are ascribed to (003) and (006) planes (Fig. 1a). The basal spacing value of  $d_{003} = 0.886 \text{ nm}$  is consistent with the presence of

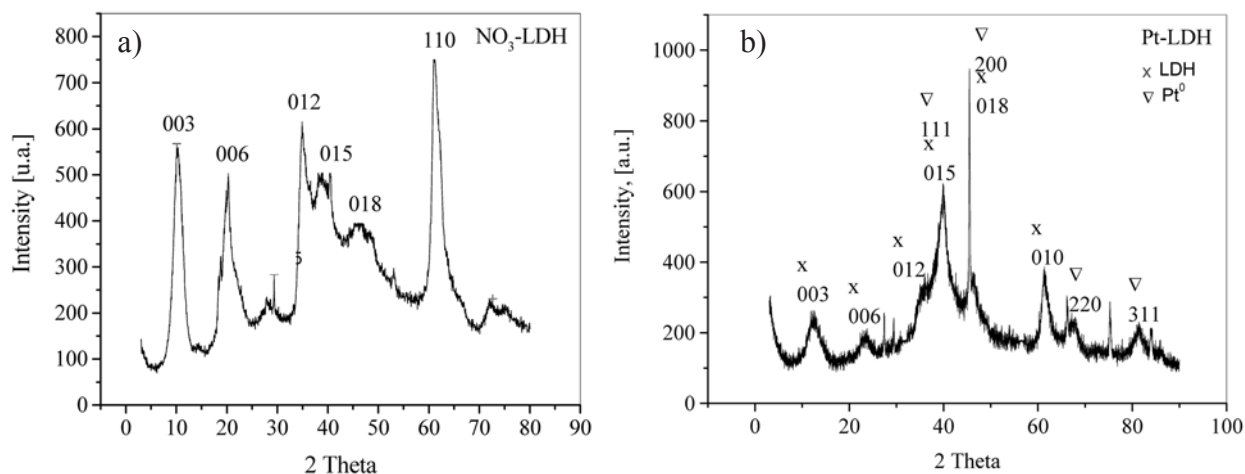


Fig. 1. XRD patterns of NO<sub>3</sub>-LDH (a) and Pt-LDH nanocomposite (b)

nitrate as charge compensating anions in the interlayer space. Compared to the XRD patterns of the host LDH, those of the Pt colloid-exchanged LDH show several changes. The crystallinity greatly decreases indicating a lower ordering in the structural arrangement (Fig. 1b). At the same time the interlayer spacing  $d_{003}$  decreases from 0.886 to 0.706 nm, even less than that in the CO<sub>3</sub><sup>2-</sup> – Mg/Al LDH ( $d_{003}$  = 0.760 nm) where the carbonate anion is the compensating anion in the interlayer space [15]. The reflections of metallic platinum are considerably broad (Fig. 1b), which indicates the formation of nanoparticles of the metal.

Thermal decomposition of both NO<sub>3</sub>-LDH and Pt-LDH nanocomposite has been studied by DTA-TG analysis (Fig. 2) under dynamic air atmosphere.

As it can be seen, three regions of mass losses from TG curves are observed, corresponding to different events in DTA profiles: dehydration, dehydroxylation and interlayer anion decomposition [15, 16]. The first weight loss, taking place between room temperature and 200 °C appears as a continuous step. It corresponds to a broad endothermic peak of H<sub>2</sub>O release and accounts for the physisorption and interlayer water molecules. The second weight loss takes place between 200 and 300 °C and associates to an endothermic peak. This corresponds to the partial dehydroxylation of the brucite-like layers. A third step in the TG plots occurs between 300 and 600 °C. It gives a broad endothermic event corresponding to the full dehydroxylation of the layer and the nitrate decomposition in the case of NO<sub>3</sub>-LDH

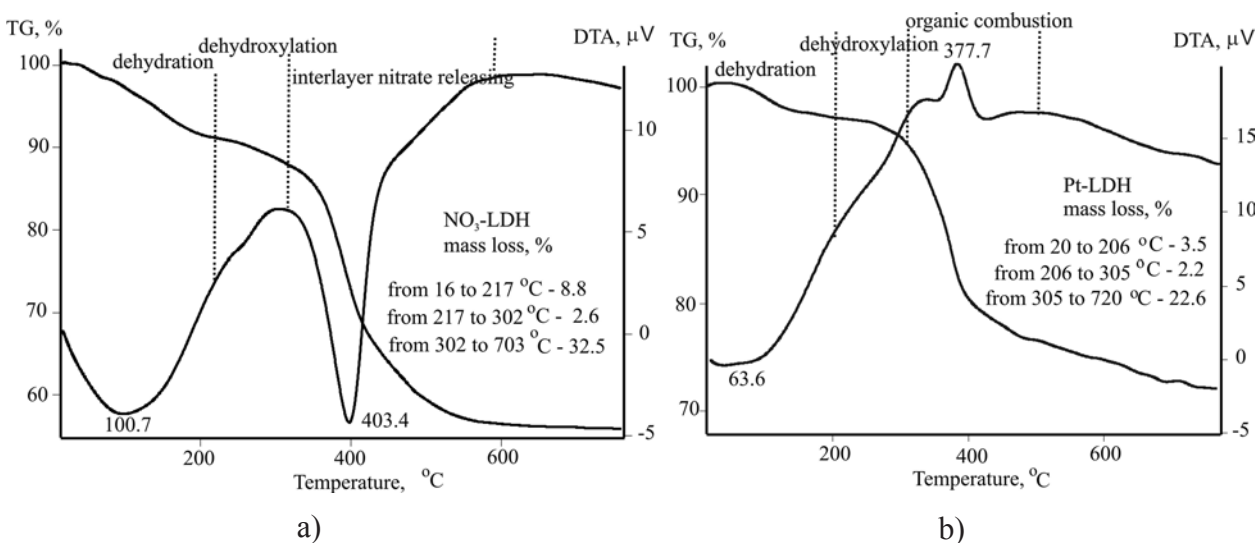


Fig. 2. DTA-TG of NO<sub>3</sub>-LDH (a) and Pt-LDH nanocomposite (b)

(Fig. 2a), while in the case of Pt- nanocomposite an exothermic event is observed corresponding to the citrate species combustion (Fig. 2b). The amount of released both components interlayer water and volatile is higher in the case of the NO<sub>3</sub>-LDH thermal decomposition comparing to that of the Pt-LDH nanocomposite. This fact confirms the reduced interlayer distance observed in XRD patterns of the Pt-LDH nanocomposite.

IR spectrum of the Pt-LDH nanocomposite presented on Figure 3 allows to identify bands associated with water and those associated with hydroxyl stretching vibrations. Water bending modes are situated around 1630 cm<sup>-1</sup> accompanied by OH-stretching vibrations in the 3000–4000 cm<sup>-1</sup> region.

The lower wavenumber region of the infrared spectrum, 1000–400 cm<sup>-1</sup>, is complicated due to the presence of lattice translational modes, librational modes of hydroxyl and water molecules, and O-M-O near 450 cm<sup>-1</sup> [17]. Meanwhile, there are absorption bands, ν<sub>3</sub> at 1385 and 1420 cm<sup>-1</sup>, which are associated with the symmetric vibration of the anionic carboxylate functions (–CO<sub>2</sub><sup>-</sup>) of the interlayer citrate-complex. In addition, the broad and strong absorption band around 1630–1580 cm<sup>-1</sup> centered

at 1632 cm<sup>-1</sup> should actually be associated with a superposition of water deformation, δ (H<sub>2</sub>O), and anti-symmetric vibration of the anionic carboxylate functions (–CO<sub>2</sub><sup>-</sup>). Di Cosimo et al. [18] have reported unidentate carbonate exhibited a symmetric O-C-O stretching vibration at 1360–1400 cm<sup>-1</sup> and an asymmetric O-C-O stretching vibration at 1510–1560 cm<sup>-1</sup>. These features correspond to the C<sub>2v</sub> carbonate group symmetry. Obviously, these groups became parts of both the interlayer and brucite-like layer. The interlayer contraction can be explained by the grafting of interlayer organic anions onto the hydroxylated layers through the substitution of OH groups on the layers. Such grafting process of organic Gly molecules on the hydroxylated layers of LDHs with a strong ion-covalent M–O-organic bonding has been reported [19] after moderate hydrothermal treatment.

*Characterization of PtNPs shape transformations and size distribution at room temperature, 500 and 1000 °C*

XRD patterns of Pt nanocomposites after heat treatment are presented on Fig. 4. The layer structure

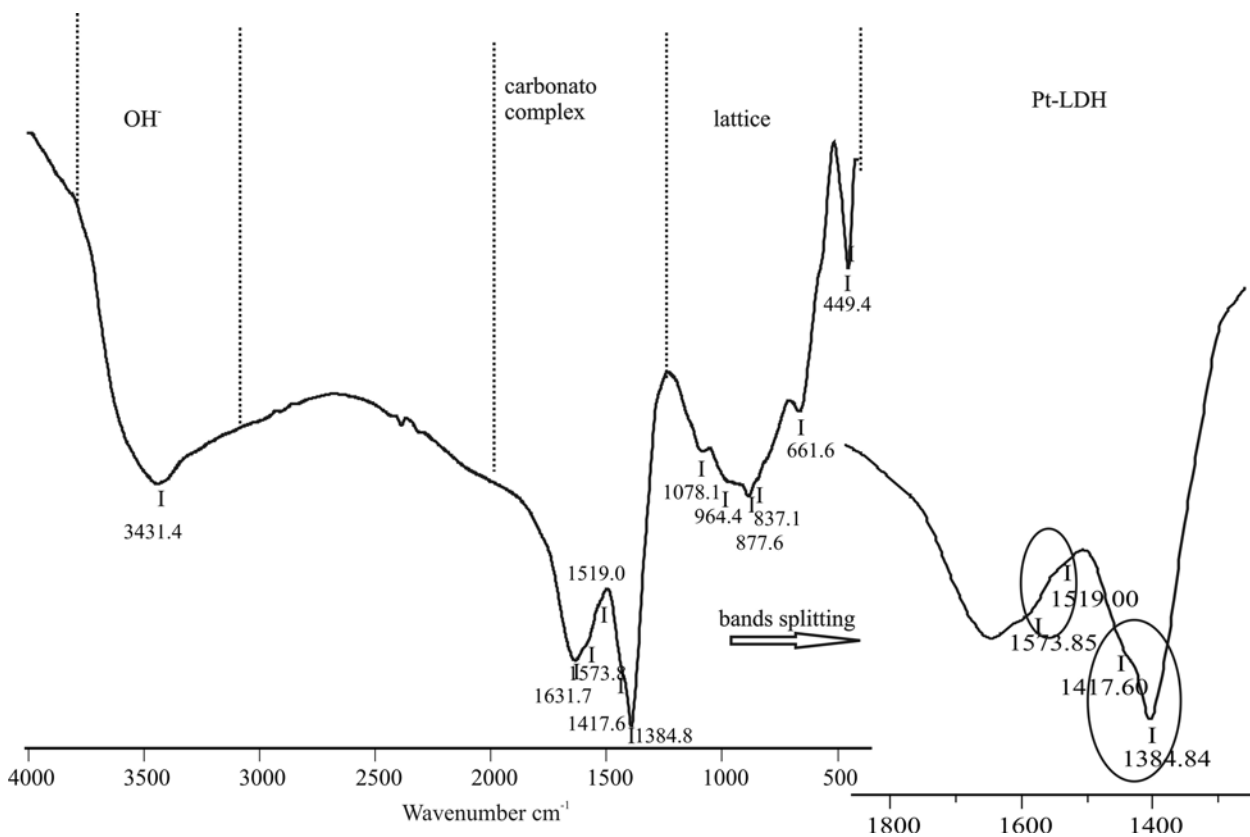


Fig. 3. IR spectrum of the Pt-LDH nanocomposite

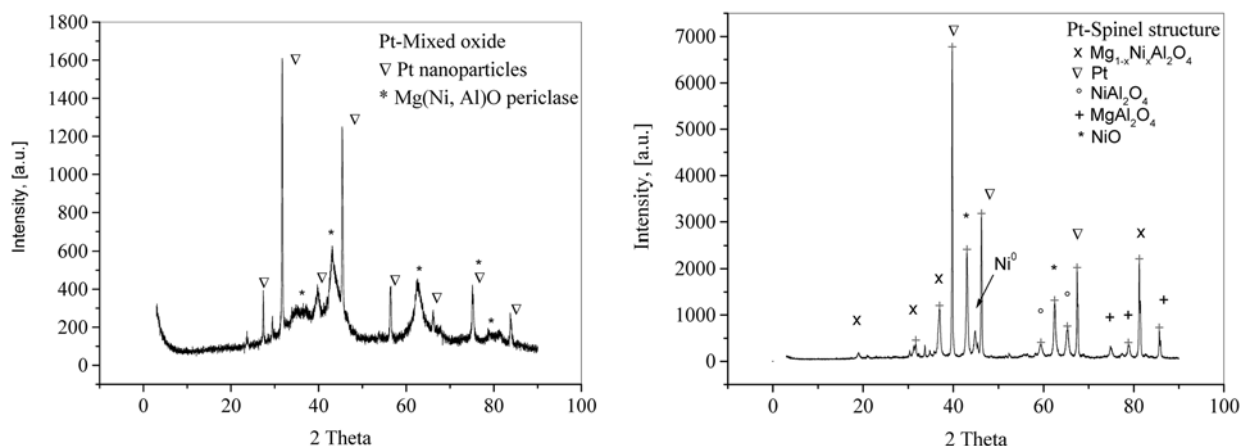


Fig. 4. XRD patterns of Pt- nanocomposites at 500 (a) and 1000 °C (b)

of the nanocomposite (Fig. 1b) transforms into mixed oxide (Fig. 4a) and spinel-like structure (Fig. 4b) at 500 and 1000 °C, respectively. At the same time, the reflections of metallic platinum become sharp, which indicates increasing of both the size and crystallinity of Pt particles with the heating temperature.

The microstructure of Pt nanocomposites, treated at the different temperatures is visualized on Fig. 5, where the bright field micrographs and corresponding SAED patterns as insets are presented. The phase composition identification confirms the presence of metal Pt phase in all three cases. A substantial increase of the mean Pt particle size is established as in [20]. The corresponding size distributions are presented on Fig. 6. The mean diameter is estimated to be 4 nm for the PtNPs at room temperature, 6 nm

at 500 °C and about 120 and 200 nm at 1000 °C. It is seen that not only the size of the PtNPs, but their shape was also changed under the heating. Initially spherical, the particles intercalated in the support coalesced, thus forming rough and granular aggregates, still spherical at 500 °C while large, dense and well-faceted, particles appeared at 1000 °C. The last ones exhibit a shape anisotropy consisting of two different dimensions in the two mutually perpendicular directions. For more of the particles one of these dimensions was significantly larger than the other. To characterize this anisotropy, two independent measurements in the two perpendicular directions for each Pt NP, annealed at 1000 °C were performed. As a result two groups of columns on the histogram were formed – one between 100 and 150 nm, correspond-

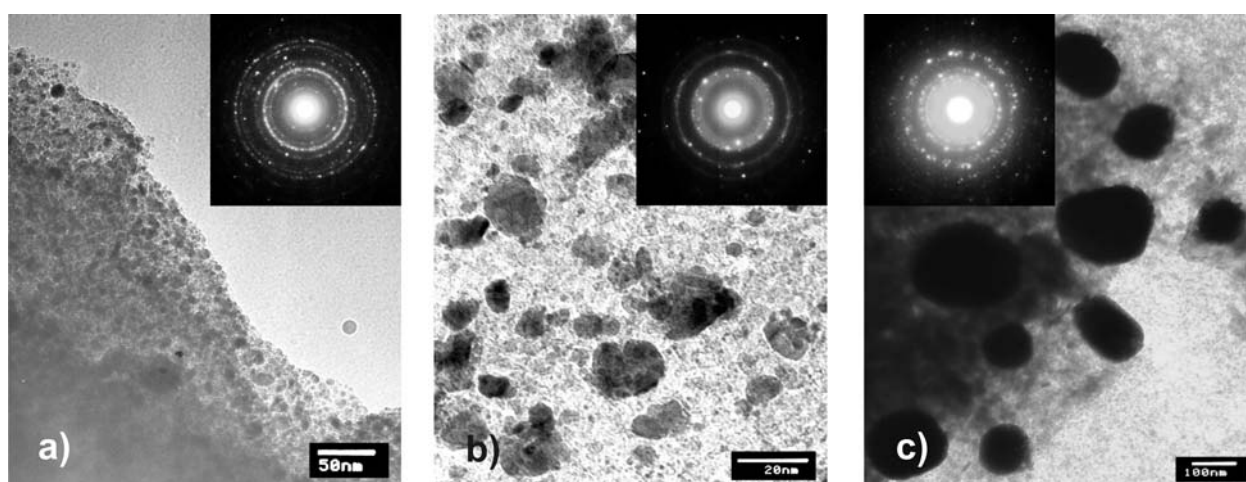


Fig. 5. Bright field TEM images and corresponding SAED patterns of Pt nanocomposites at room temperature (a), 500 °C (b) and 1000 °C (c)

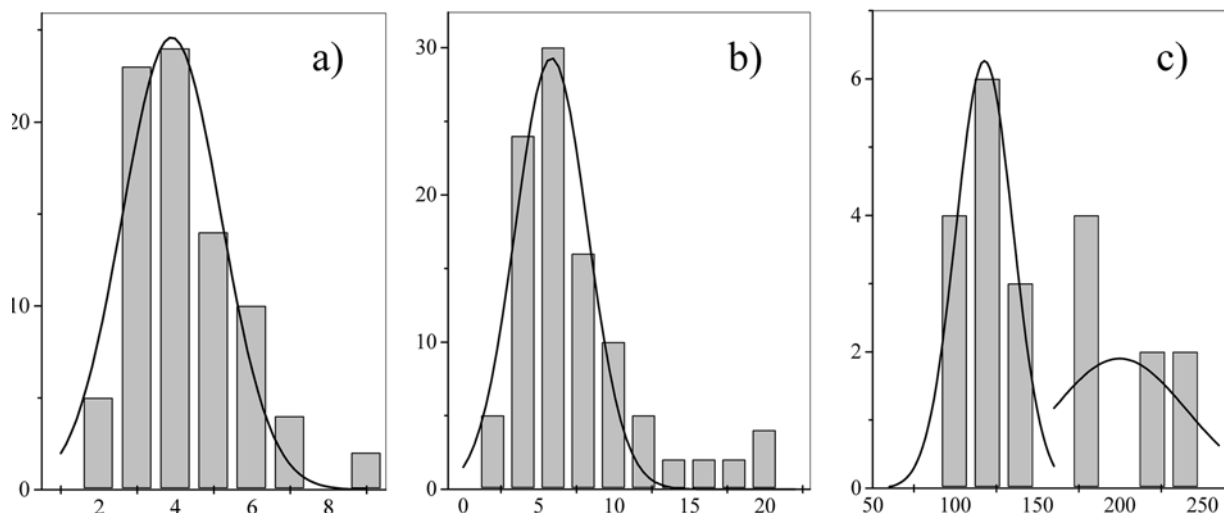


Fig. 6. Size distributions of PtNPs in the samples presented on Fig. 5

ing to the less dimension and one between 180 and 240 nm, due to the larger dimension.

### CONCLUSIONS

An effective method for synthesis of PtNPs based nanocomposite as a promising material for catalytic applications was established. A thermal treatment for size and microstructure fine control of the PtNPs was applied. It was observed that intercalated in the precursor PtNPs were coalesced becoming dense and well-faced under heating. Thus, the layer structure of the catalytic nanocomposite favors in best way the fine distribution and nanosize control of the Pt particles.

### REFERENCES

1. A. Vaccari, *Appl. Clay Sci.*, **14**, 161 (1999).
2. D. Tichit, B. Coq, B. Cattech, **7**, 206 (2003).
3. S. Narayanan, *Bulletin of the Catalysis Society of India*, **2**, 107 (2003).
4. F. Cavani, F. Trifiro, A. Vaccari, *Catal. Today*, **11**, 173 (1991).
5. A. De Roy, C. Forano, K. El Malki, J. P. Besse, in: *Synthesis of Microporous Materials*, M. L. Occelli, H. Robson (eds.), Van Nostrand Reinhold: New York, 1992, p. 108.
6. V. Rives, *Layered Double Hydroxides: Present and Future*, V. Rives (ed.), Nova Science Publishers: New York, 2001, p. 115.
7. F. Basile, L. Basini, G. Fornasari, M. Gazzano, F. Trifiro, A. Vaccari, *J. Chem. Soc., Chem. Commun.*, 2435 (1996).
8. F. Basile, G. Fornasari, M. Gazzano, A. Vaccari, *Appl. Clay Sci.*, **16**, 185 (2000).
9. M. K. Titulaer, J. Ben, H. Jansen, J. Geus, *Clays Clay Miner.*, **42**, 249 (1994).
10. C. Gerardin, D. Kostadinova, N. Sanson, D. Francova, N. Tanchoux, D. Tichit, B. Coq, *Stud. Surf. Sci. Catal.*, **156**, 357 (2005).
11. V. Rives, M. Ulibarri, *A. Coord. Chem. Rev.*, **61**, 181 (1999).
12. J. Turkevich, P. Stevenson, J. Hillier, *Discuss. Faraday Soc.*, **11**, 55 (1951).
13. A. Harriman, G. R. Millward, P. Neta, M. C. Richoux, J. M. Thomas, *J. Phys. Chem.*, **92**, 1286 (1988).
14. D. Kostadinova, G. Topalov, A. Stoyanova, E. Lefterova, I. Dragieva, *Bulgarian Chemical Communications*, **43**, 1, 150 (2011).
15. Ts. Stanimirova, I. Vergilov, G. Kirov, N. Petrova, *J. Mater. Sci.*, **34**, 4153 (1999).
16. C. Ge'ardin, D. Kostadinova, N. Sanson, B. Coq, D. Tichit, *Chem. Mater.*, **17**, 6473 (2005).
17. S. J. Palmer, L. Frost, T. Nguen, *Coordination Chemistry Reviews*, **253**, 250 (2009).
18. J. I. Di Cosimo, V. K. Diez, M. Xu, E. Iglesia, C. R. Apesteguia, *J. Catal.*, **178**, 499 (1998).
19. F. Li, L. Zhang, D. G. Evans, C. Forano, X. Duan, *Thermoch. Acta*, **424**, 15 (2004).
20. A. V. Lukashin, M. V. Chernysheva, A. A. Vertegel, Yu. D. Tret'yakov, *Doklady Chemistry*, **388**, 1-3, 19 (2003).

## РАЗМЕР И РАЗПРЕДЕЛЕНИЕ НА Pt НАНОЧАСТИЦИ В LDH НАНОКОМПОЗИТИ ПРИ РАЗЛИЧНИ ТЕМПЕРАТУРИ

Д. Б. Карашанова<sup>1\*</sup>, Д. Д. Костадинова<sup>2</sup>, С. В. Василев<sup>2</sup>, Н. Л. Петрова<sup>3</sup>

<sup>1</sup> *Институт по оптически материали и технологии „Акад. Йордан Малиновски“,  
Българска академия на науките, 1113 София, България*

<sup>2</sup> *Институт по електрохимия и енергийни системи, Българска академия на науките,  
1113 София, България*

<sup>3</sup> *Институт по минералогия и кристалография, Българска академия на науките,  
1113 София, България*

Постъпила на 15 февруари, 2012 г.; приета на 17 април, 2012 г.

(Резюме)

Успешно са синтезирани нанокomпозити от мултикатионни слоисти двойни хидроксиди (LDH) и платиновни наночастици (PtNPs). Слоистата структура на нанокomпозитите е охарактеризирана с рентгенова дифракция (XRD) и инфрачервена (IR) спектроскопия, а термичните им свойства – посредством диференциален термичен и термогравиметричен (DTA-TG) анализ. Установено е свиване на междуслойното пространство, което може да бъде обяснено с вграждането на органичните аниони, разположени там, в хидроксилираните слоеве. С помощта на трансмисионна електронна микроскопия (ТЕМ) е наблюдавана промяната на размера и разпределението на PtNPs след термично третиране на образците при 500 °С и 1000 °С. В резултат на нагряването, интеркалираните в подложката PtNPs коалесцират. При стайна температура те са сферични и силно диспергирани по повърхността на подложката, докато при 500 °С се групират в агрегати с неправилна форма, а при 1000 °С се трансформират в големи, плътни и добре остенени частици.